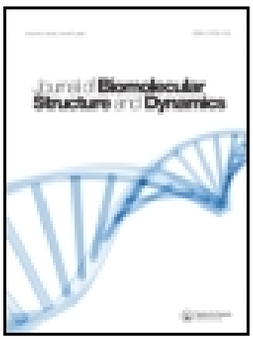

Taylor & Francis
Taylor & Francis Group

Journal of Biomolecular Structure and Dynamics

ISSN: (Print) (Online) Journal homepage: https://www.tandfonline.com/loi/tbsd20

N-substituted benzenesulfonamide compounds: DNA binding properties and molecular docking studies

Seyit Ali Güngör, Mehmet Tümer, Muhammet Köse & Sultan Erkan

To cite this article: Seyit Ali Güngör, Mehmet Tümer, Muhammet Köse & Sultan Erkan (2021): N-substituted benzenesulfonamide compounds: DNA binding properties and molecular docking studies, Journal of Biomolecular Structure and Dynamics, DOI: 10.1080/07391102.2021.1897683

To link to this article: https://doi.org/10.1080/07391102.2021.1897683

JOURNAL OF BIOMOLECULAR STRUCTURE AND DYNAMICS
https://doi.org/10.1080/07391102.2021.1897683

N-substituted benzenesulfonamide compounds: DNA binding properties and molecular docking studies

Seyit Ali Güngör[a], Mehmet Tümer[a], Muhammet Köse[a] and Sultan Erkan[b]

[a]Chemistry Department, K.Maras Sütcü Imam University, K.Maras, Turkey; [b]Department of Chemistry and Chemical Processing Technologies, Sivas Cumhuriyet University Yıldızeli Vocational School, Sivas, Turkey

Communicated by Ramaswamy H. Sarma

ABSTRACT

Benzenesulfonamide-based imine compounds **5**–**8** were prepared and screened for their binding properties to the FSdsDNA. The structures of synthesized compounds were elucidated by the spectroscopic and analytical methods. Compounds **5**–**8** were screened for their interactions with the FSdsDNA. Compound **8** showed the highest binding affinity to the FSdsDNA with intrinsic binding constant of 3.10×10^4 M^{-1}. The compounds caused the quenching of the DNA–EB emission indicating displacement of EB (ethidium bromide) from the FSdsDNA. Finally, the binding interactions between the DNA and binder molecules **5**–**8** were examined by the molecular docking studies. The compounds locate approximately same region of the minor groove of DNA *via* hydrogen bonding contacts between the sulfonamide oxygen atoms and the DG10/DG16 nucleotides of DNA.

ARTICLE HISTORY
Received 2 December 2020
Accepted 25 February 2021

KEYWORDS
Sulfonamide; propargyl; imine; DNA; molecular docking

1. Introduction

Before penicillin was commercially available and used, many sulfonamide-derived drugs with good solubility in water were used by humans. But, the sulfonamide-based drugs used in the early times have caused many health problems. Sulfonamides have a functional group that forms the basis of several drug groups called sulfa drugs. Several organic molecules containing a sulfonamide group have been prepared and their structures have been characterized. The chemical, physical and biological properties (antibacterial, antifungal, diuretic, anticarbonicanhydrase, antithyroid, hypoglycemic, antitumour, etc.) of these compounds have also been investigated (Davenport, 2012; Drews, 2000; Durgun et al., 2016; Jaiswal et al., 2004; Krátký et al., 2012). Original antibacterial sulfonamides are synthetic (non-antibiotic) and they contain the sulfonamide group (Henry, 1943). Since the sulfonamide-based compounds have different biological properties, the biological properties of such compounds have been extensively studied. For example, sulfonamide compounds are often used for the prevention and treatment of bacterial infections in humans. The interactions with DNA of sulfonamides have been studied since for a long time. In many studies, it has been determined that the substituted groups on the ring of sulfonamides affect the interactions with DNA (Dixit et al., 2011; García-Giménez et al., 2013; Rajendiran & Thulasidhasan, 2015). It was determined that the Cu(II) complexes of sulfonamides interact more strongly with DNA than free ligand (García-Giménez et al., 2013).

Investigation of the interactions between DNA or other biomolecules and small molecules is the key to design new drugs for the treatment of several diseases (Boer et al., 2009; Horiuchi, 2002). Small molecules can bind to DNA *via* covalent or non-covalent interactions (Mokaberi et al., 2020). DNA molecules have several type of binding sites and the interaction between drug molecules and DNA can cause DNA damage in cancer cells. The type of interactions depends mainly on the size, conformation and the functional groups in the binding molecules. The interactions between the certain molecule and DNA can be investigated by experimental (UV–vis absorption and emission) and docking studies (Tumer et al., 2017). The change in the absorption wavelengths and intensities of the DNA binding agents can give a clue about the possible binding mode. The hyperchromic and hypochromic shifts, for example, in the absorption bands are indicative of changes in minor or major distortions in DNA conformation. The hyperchromic shift is usually attributed to the breakage of the secondary structure of DNA *via* binding agent.

Schiff bases are one of the most easily synthesized compounds and they are usually obtained from the condensation reaction of the aromatic or aliphatic primary amines and the carbonyl compounds (especially aromatic aldehydes) (Basak & Ray, 2020; Golcu et al., 2005; Wang et al., 2020). Schiff bases are organic in nature and contain heteroatoms such as nitrogen, oxygen or sulphur in their nature. For this reason, these compounds have important biological properties. For example, Schiff bases have found numerous applications

CONTACT M. Tumer mtumer@ksu.edu.tr; S.A. Gungor sagungor@ksu.edu.tr Chemistry Department, K.Maras Sütcü Imam University, K.Maras 46100, Turkey

Supplemental data for this article can be accessed online at https://doi.org/10.1080/07391102.2021.1897683

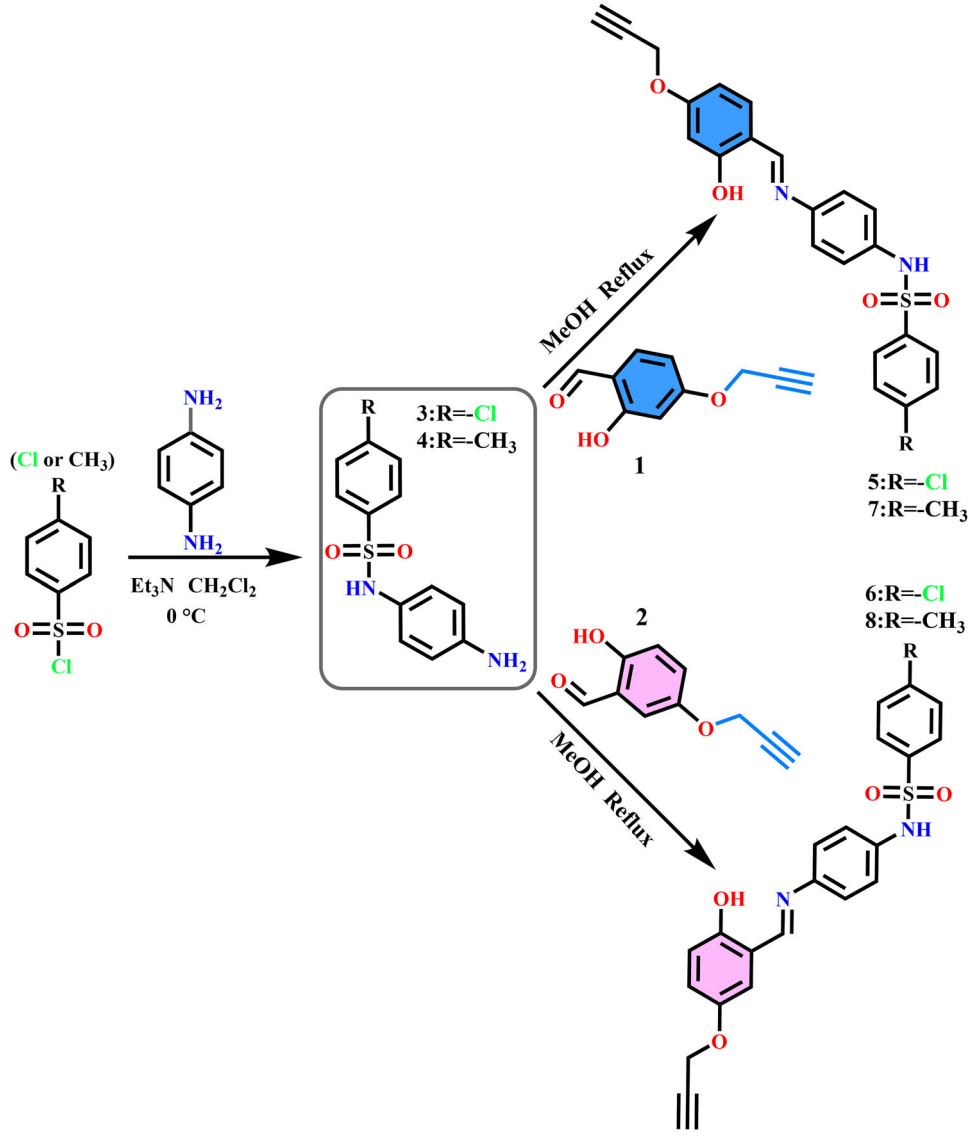

Scheme 1. Synthesis reactions of the sulfonamide-based compounds.

such as microbiological, insecticidal, anticancer, antiviral and dye compound (Marchetti et al., 2015, 2019; Pahontu et al., 2015; Tajudeen & Kannappan, 2016). On the other hand, Schiff bases are also suitable for applications such as chemosensors and gas sensors (Doğan et al., 2020; Formica et al., 2018; Wei et al., 2019; Xing et al., 2018).

In the current work, two sulfonamide amine derivatives (**3** and **4**) and four sulfonamide-based imine compounds **5**–**8** were prepared and characterized their structures using the spectroscopic and analytical techniques. Molecular structures of compounds **3**, **5**–**7** were identified by the X-ray diffraction studies. To review the keto-enol tautomeric forms of compounds **5**–**8**, their electronic properties have studied in the polar and a polar solvents. The synthesized sulfonamide-based Schiff base compounds were screened for their binding affinities towards FSdsDNA (fish sperm double strand DNA) by using spectrophotometric techniques. Finally, the binding modes of the compounds with DNA were investigated by molecular docking studies.

2. Methods and material

Physical measurements, preparation and characterization data for the starting compounds [carbonyls (**1**, **2**) and N-substituted benzenesulfonamides (**3**, **4**)] were provided in the Supplementary File. The X-ray crystallographic data collection and refinement details, molecular docking and DNA binding procedures have also been given in the Supplementary File.

2.1. Preparation of the sulfonamide-based Schiff base compounds 5–8

The N-substituted benzenesulfonamides **3** or **4** (1 mmol) were dissolved in methanol (15 mL). The carbonyl compounds **1** or **2** (1 mmol) dissolved in MeOH (15 mL) were added to the sulfonamide solution. The mixture was refluxed for 5–6 h and cooled to room temperature. The precipitates were filtered and dried in a vacuum desiccator. The obtained compounds were recrystallized from methanol.

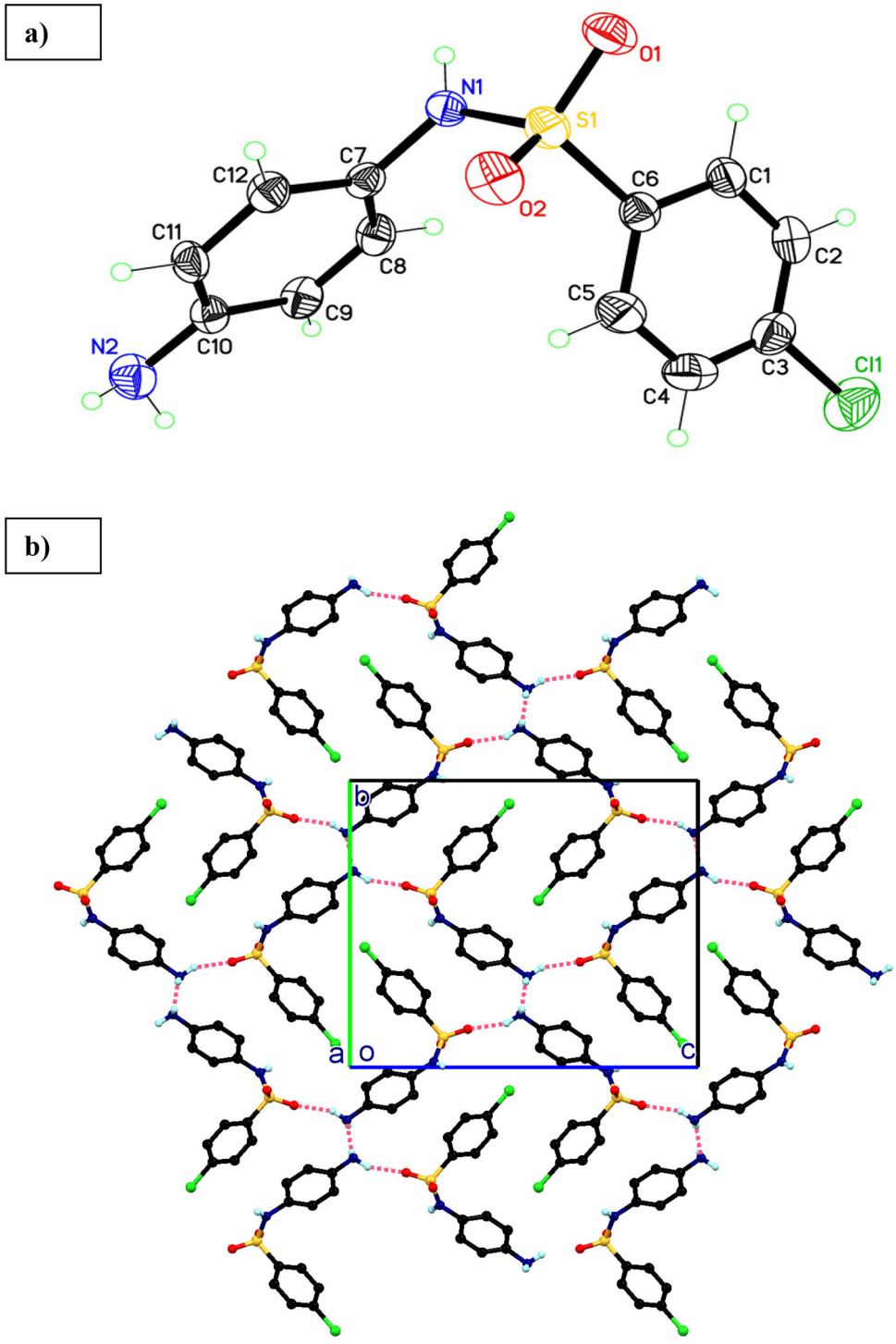

Figure 1. (a) Molecular structure of **3** with thermal ellipsoid 30% probability. (b) Packing diagram of **3** viewing down the *a* axis showing 2D hydrogen bond network.

5: $C_{22}H_{17}ClN_2O_4S$. Yield: 88%, Color: Light orange, Mp: 156–158 °C. Elemental analysis; found (Calculated) %: C, 58.34 (59.93); H, 3.90 (3.89); N, 6.36 (6.35); S 7.52 (7.27). ^{1}H NMR (d_6-DMSO, ppm): δ 13.57 (s, 1H), 10.47 (s, 1H), 8.80 (s, 1H), 7.76 (d, 2H), 7.65 (d, 2H), 7.51 (d, 1H), 7.30 (d, 2H), 7.14 (d, 2H), 6.58 (d, 1H), 6.54 (s, 1H), 4.86 (s, 2H), 3.63 (s, 1H). ^{13}C NMR: δ 163.14, 162.46, 161.82, 144.69, 138.64, 138.34, 136.17, 134.43, 129.95, 129.09, 122.56, 121.97, 113.93, 107.78, 102.26, 79.25, 79.09, 56.15. IR (ν, cm^{-1}): 3274 ν(−OH), 3237 ν(−NH), 2116 ν(–C≡C–), 1615 ν(–**C = N**–), 1333 and 1155 ν(–SO_2). Mass ESI-MS (*m/z*): Calculated 440.06, found 440.10 $[C_{22}H_{17}ClN_2O_4S]^+$.

6: $C_{22}H_{17}ClN_2O_4S$. Yield: 84%, Color: Dark orange, Mp: 131–133 °C. Elemental analysis; found (Calculated) %: C, 58.48 (59.93); H, 3.94 (3.89); N, 6.31 (6.35); S 7.41 (7.27). ^{1}H NMR (d_6-DMSO, ppm): δ 12.43 (s, 1H), 10.49 (s, 1H), 8.83 (s,

Table 1. Crystallographic data for the compounds.

Identification code	3	5	6	7
Empirical formula	$C_{12}H_{11}ClN_2O_2S$	$C_{22}H_{17}ClN_2O_4S$	$C_{22}H_{17}ClN_2O_4S$	$C_{23}H_{20}N_2O_4S$
Crystal size	0.17 × 0.12 × 0.09	0.14 × 0.10 × 0.07	0.17 × 0.11 × 0.07	0.18 × 0.12 × 0.08
Crystal colour	Colorless	Yellow	Yellow	Yellow
Formula weight	282.74	440.88	440.88	420.47
Crystal system	*Orthorhombic*	*Monoclinic Monoclinic*	*Triclinic*	*Monoclinic*
Space group	$P2_12_12_1$	*P 1 21/c1*	*P-1*	*P 1 21/c 1*
Unit cell *a* (Å)	4.9961(3)	23.3986(16)	6.239(2)	11.9692(3)
b (Å)	14.7657(12)	11.1632(7)	8.2368(10)	11.1727(3)
c (Å)	17.9014(12)	16.0504(11)	20.167(3)	16.1300(4)
α (°)	90	90	91.669(10)	90
β (°)	90	96.863(6)	90.94(2)	95.627(2)
γ (°)	90	90	102.68(2)	90
Volume (Å3)	1320.60(16)	4162.4(5)	1010.4(4)	2146.64(10)
Z	4	8	2	4
Abs. coeff. (mm^{-1})	0.442	0.316	0.325	0.182
Refl. collected	3138	14412	7508	8911
Completeness to theta	99.1%	98.9 %	99.6%	99.8%
Ind. Refl. [R_{int}]	2344 [0.0187]	8284[0.0326]	4552 [0.0685]	4883 [0.0183]
*R*1, *wR*2 [$I > 2\sigma(I)$]	0.0488, 0.0899	0.0659, 0.1272	0.0788, 0.1815	0.0512, 0.1242
*R*1, *wR*2 (all data)	0.0770, 0.10227	0.1423, 0.1605	0.2112, 0.2828	0.0769, 0.1432
CCDC	1990864	1990865	1990866	1990867

1H), 7.77 (d, 2H), 7.65 (d, 2H), 7.32 (d, 2H), 7.27 (s, 1H), 7.16 (d, 2H), 7.09 (d,1H), 6.90 (d, 1H), 4.76 (s, 2H), 3.57 (s, 1H). ^{13}C NMR: δ 162.47, 155.24, 150.20, 145.00, 138.65, 138.36, 136.63, 129.97, 129.09, 122.82, 121.82, 121.67, 119.68, 117.84, 117.45, 79.82, 78.73, 56.61. IR (ν, cm^{-1}): 3292 ν(−OH), 3260 ν(−NH), 2110 ν(–C≡C–), 1620 ν(–**C = N**–), 1338 and 1158 ν(–SO_2). Mass ESI-MS (*m/z*): Calculated 440.06, found 440.25 $[C_{22}H_{17}ClN_2O_4S]^+$.

7: $C_{23}H_{20}N_2O_4S$. Yield: 86%, Color: Light orange, Mp: 172–175 °C. Elemental analysis; found (Calculated) %: C, 63.71 (65.70); H, 4.89 (4.79); N, 6.93 (6.66); S 7.67 (7.62). ^{1}H NMR (d_6-DMSO, ppm): δ 13.60 (s, 1H), 10.33 (s, 1H), 8.79 (s, 1H), 7.66 (d, 2H), 7.50 (d, 1H), 7.35 (d, 2H), 7.28 (d, 2H), 7.15 (d, 2H), 6.58 (d, 1H), 6.54 (s, 1H), 4.86 (s, 2H), 3.64 (s, 1H), 2.33 (s, 3H). ^{13}C NMR: δ 163.13, 162.26, 161.77, 144.23, 143.79, 137.01, 136.72, 134.38, 130.19, 127.19, 122.46, 121.39, 113.93, 107.76, 102.25, 79.26, 79.12, 56.15, 21.42. IR (ν, cm^{-1}): 3303 ν(−OH), 3282 ν(−NH), 2122 ν(–C≡C–), 1614 ν(–**C = N**–), 1335 and 1156 ν(–SO_2). Mass ESI-MS (*m/z*): Calculated 420.11, found 422.18 $[C_{23}H_{20}N_2O_4S + 2H]^+$.

8: $C_{23}H_{20}N_2O_4S$. Yield: 83%, Color: Orange, Mp: 143–145 °C. Elemental analysis; found (Calculated) %: C, 63.93 (65.70); H, 4.94 (4.79); N, 7.07 (6.66); S 7.63 (7.62). ^{1}H NMR (d_6-DMSO, ppm): δ 12.46 (s, 1H), 10.36 (s, 1H), 8.83 (s, 1H), 7.67 (d, 2H), 7.36 (d, 2H), 7.30 (d, 2H), 7.26 (d, 1H), 7.16 (d, 2H), 7.08 (dd, 1H), 6.90 (d, 1H), 4.75 (s, 2H), 3.57 (s, 1H), 2.34 (s, 3H). ^{13}C NMR: δ 183.95, 162.26, 155.24, 150.19, 144.54, 143.82, 137.15, 137.01, 130.21, 127.19, 122.72, 121.60, 121.24, 119.69, 117.82, 117.46, 79.83, 78.72, 56.61, 21.42. IR (ν, cm^{-1}): 3303 ν(−OH), 3261 ν(−NH), 2105 ν(–C≡C–), 1621 ν(–**C = N**–), 1332 and 1151 ν(–SO_2). Mass ESI-MS (*m/z*): Calculated 420.11, found 421.80 $[C_{23}H_{20}N_2O_4S + H]^+$.

3. Results and discussions

In this work, two N-substituted benzenesulfonamide-based starting materials **3** and **4** have been obtained from the reaction of the 4-chloro (or 4-methyl) benzenesulfonyl chloride and p-phenylenediamine at low temperature (Scheme 1). The carbonyl compounds **1** and **2** that were used to synthesize the sulfonamide-based Schiff base compounds **5–8** have previously obtained and characterized by our group (Güngör et al., 2020). These compounds have prepared from the reaction of the 4-hydroxy and 5-hydroxy salicylaldehyde carbonyl compounds and 3-bromopropyne in acetonitrile (Güngör et al., 2020). From the reaction of the N-(4-aminophenyl)-4-benzenesulfonamide derivatives (**3**, **4**) and the carbonyl compounds (**1**, **2**) in the ethanol solution, we have prepared the sulfonamide-based Schiff base compounds (**5–8**). The organic compounds have been characterized by using the elemental analyses, mass (LC–MS), ^{1}H(^{13}C) NMR, UV–vis, photoluminescence and FTIR methods. The single crystals of compounds **3, 5–7** were grown and their solid structures were further determined by the X-ray crystallography.

The ^{1}H(^{13}C) NMR spectra of compounds **3–8** were recorded in d_6-DMSO solvent. The ^{1}H(^{13}C) NMR spectra of the compounds are provided in the Supplementary Documents. In the ^{1}H NMR spectra of compounds **3** and **4**, the signals at 9.56 and 9.40 ppm come from the amide proton (–NH–C = O). The multiplets in the 7.61–6.37 ppm range may be assigned to the aromatic ring hydrogen atoms (Ar–H). The hydrogen atoms of the primary –NH_2 groups on the *p*-phenylene diamine ring have been shown at 5.02 and 4.94 ppm as broad band. In compound **4**, the singlet at 2.34 ppm can be attributed to the hydrogen atoms of the –CH_3 group. The ^{13}C NMR spectra of compounds **3** and **4** show that the aromatic ring carbon atoms are in the 147.27–114.42 ppm range. The methyl group carbon atom of compound **4** is shown at 21.41 ppm.

The sulfonamide-based Schiff base compounds **5–8** showed broad peaks due to the phenolic OH in the 12.43–13.60 ppm range. The hydrogen atoms of the amide groups of the imine compounds were observed in the 10.33–10.49 ppm range. The singlets of the hydrogen atoms belonging to the imine group (–CH = N–) were shown in the 8.79–8.83 ppm range. The aromatic ring protons (Ar–H) of the imine compounds **5–8** were observed in the 6.54–7.77 ppm range as multiplet. The aliphatic hydrogen

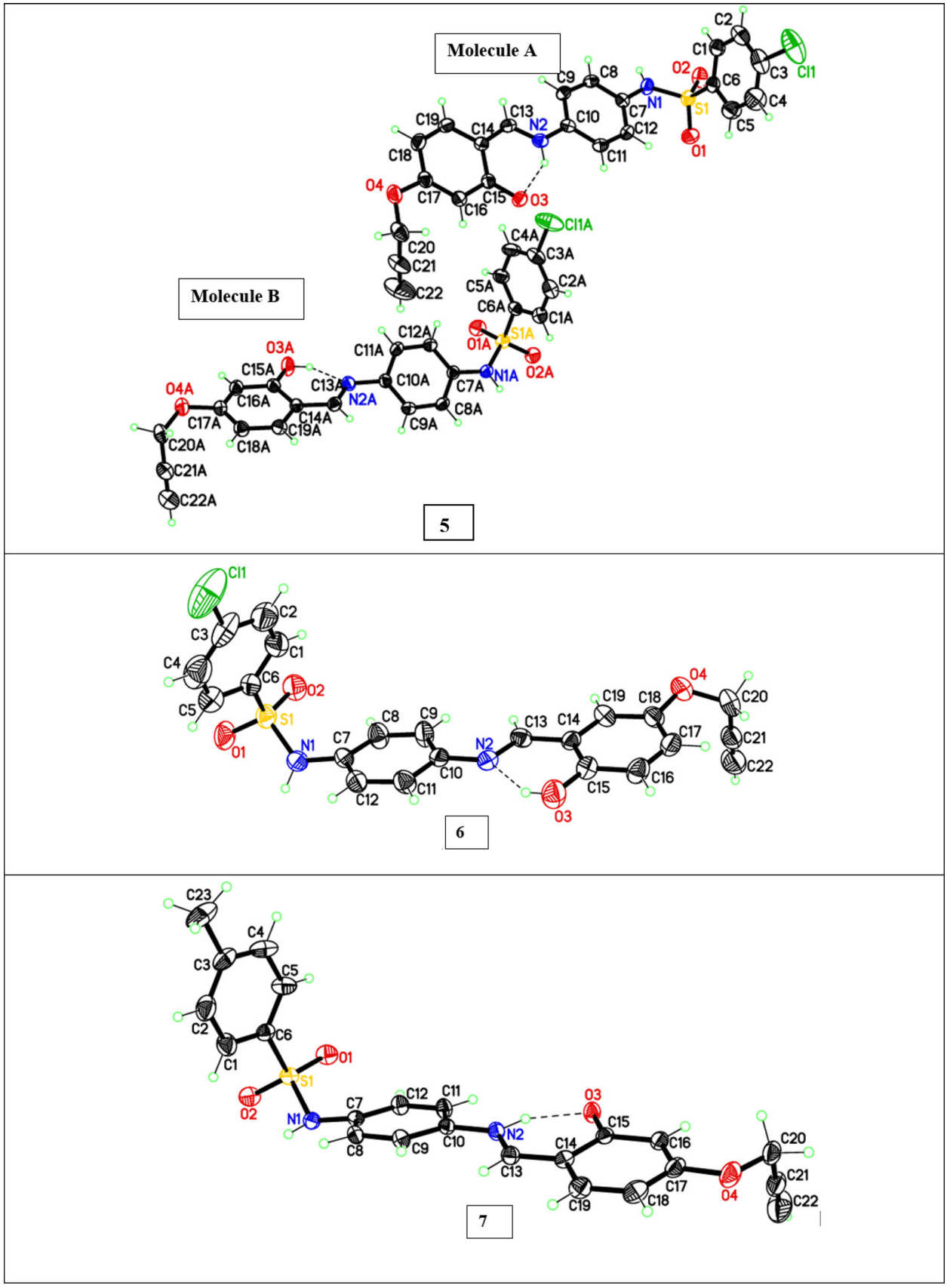

Figure 2. Asymmetric unit of **5**–**7** with thermal ellipsoid 30% probability. Two independent molecules in **5** are labelled as molecule A and B.

Table 2. Selected bond lengths (Å) and angles (°) for compounds **5**–**7**.

	5	6	7
S(1)–O(1)	1.427(3)	1.420(4)	1.4249(18)
S(1)–O(2)	1.430(3)	1.439(4)	1.4319(16)
S(1)–N(1)	1.619(3)	1.626(5)	1.6224(17)
S(1)–C(6)	1.755(4)	1.748(6)	1.764(2)
N(2)–C(13)	1.306(4)	1.281(6)	1.310(3)
O(3)–C(15)	1.299(4)	1.371(6)	1.296(2)
C(21)–C(22)	1.132(6)	1.128(8)	1.150(5)
S(1A)–O(1A)	1.427(2)	–	–
S(1A)–O(2A)	1.426(2)	–	–
S(1A)–N(1A)	1.609(3)	–	–
S(1A)–C(6A)	1.758(4)	–	–
N(2A)–C(13A)	1.293(4)	–	–
O(3A)–C(15A)	1.321(4)	–	–
C(21A)–C(22A)	1.149(6)	–	–
O(1)–S(1)–O(2)	118.31(17)	120.1(3)	119.78(11)
O(1)–S(1)–N(1)	110.58(16)	105.1(2)	108.60(10)
O(1)–S(1)–C(6)	108.03(18)	107.9(3)	108.05(11)
O(2)–S(1)–N(1)	105.31(16)	108.4(3)	104.41(10)
O(2)–S(1)–C(6)	108.53(17)	108.2(3)	107.94(11)
N(1)–S(1)–C(6)	105.33(16)	106.4(3)	107.48(10)
C(20)–C(21)–C(22)	178.4(7)	177.1(7)	178.5(5)
O(1A)–S(1A)–N(1A)	109.45(16)	–	–
O(1A)–S(1A)–C(6A)	107.74(17)	–	–
O(2A)–S(1A)–O(1A)	120.22(16)	–	–
O(2A)–S(1A)–N(1A)	105.15(15)	–	–
O(2A)–S(1A)–C(6A)	107.54(16)	–	–
N(1A)–S(1A)–C(6A)	105.89(15)	–	–
C(20A)–C(21A)–C(22A)	178.6(5)	–	–

atoms of the $-OCH_2-$ group in the imine compounds **5–8** have been determined in the 4.75–4.86 ppm range. Hydrogen atoms of the acetyl group (–C≡CH) attached to the salicylidene ring of the imine compounds have been shown in the 3.57–3.64 ppm range. In the spectra of compounds **7** and **8**, the singlets at 2.33 and 2.34 ppm belong to the hydrogen atoms of the $-CH_3$ group on the N-benzenesulfonamide rings.

In the ^{13}C NMR spectrum of compound **1**, the signals in the 164.19–115.75 ppm are due to the aromatic ring carbon atoms (Ar–C). The oxygen atoms attached to the carbon atoms attached to the *ortho*- and *para*-positions of the aromatic ring shifted the chemical shift values of the carbon atoms to the lower regions. In the ^{13}CNMR spectra of compounds **5–8**, the signals in the 164.55–162.26 ppm range are assigned to the carbon atoms of the azomethine groups. The aromatic ring carbons were observed in the 155.24–102.25 ppm range. The signals in the 79.83–78.72 ppm range can be attributed to the terminal acetylene carbon atoms (–C≡CH) of the propargyl group on the salicylidene rings. The carbon atoms of the $-OCH_2-$ group on the salicylidene rings were seen in the 56.15–56.61 ppm range. In the spectra of compounds **7** and

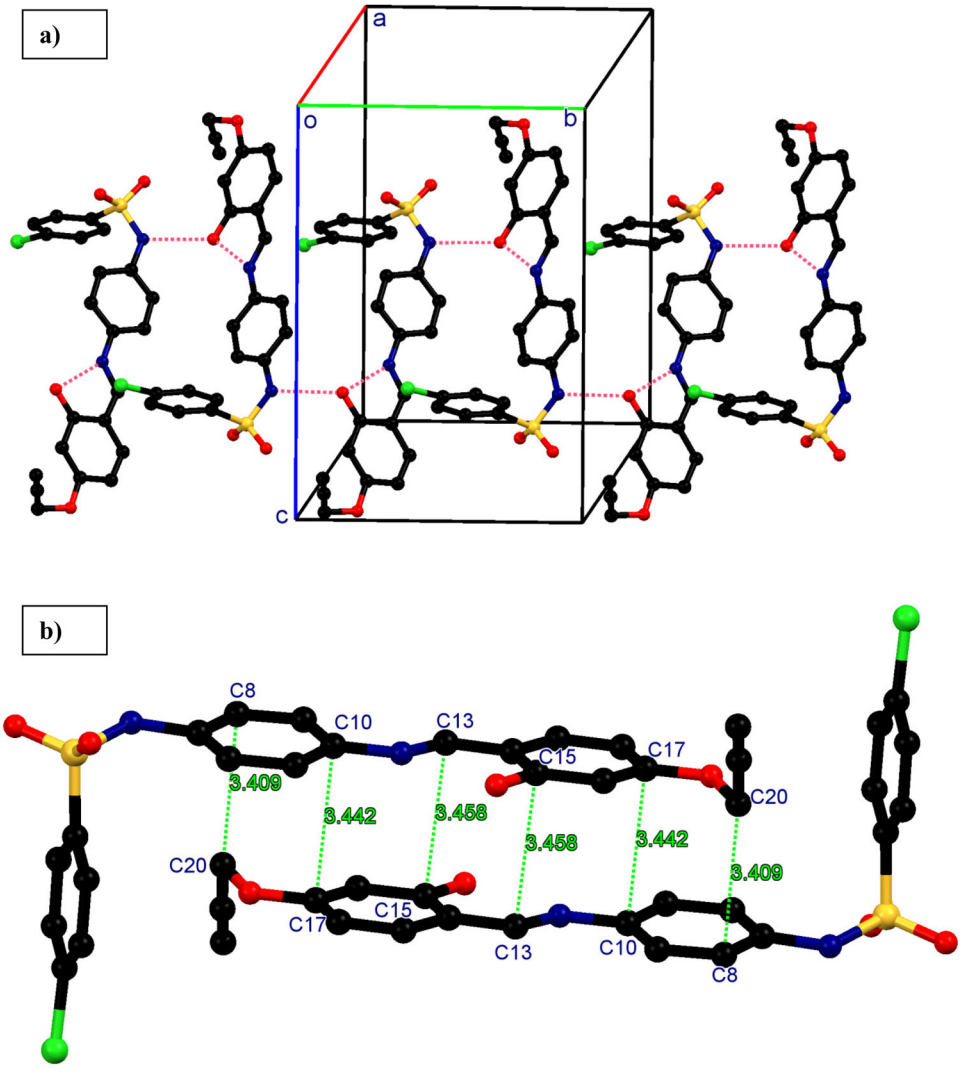

Figure 3. (a) 1D hydrogen bond chain in **5**. (b) π–π stacking interactions in **5**.

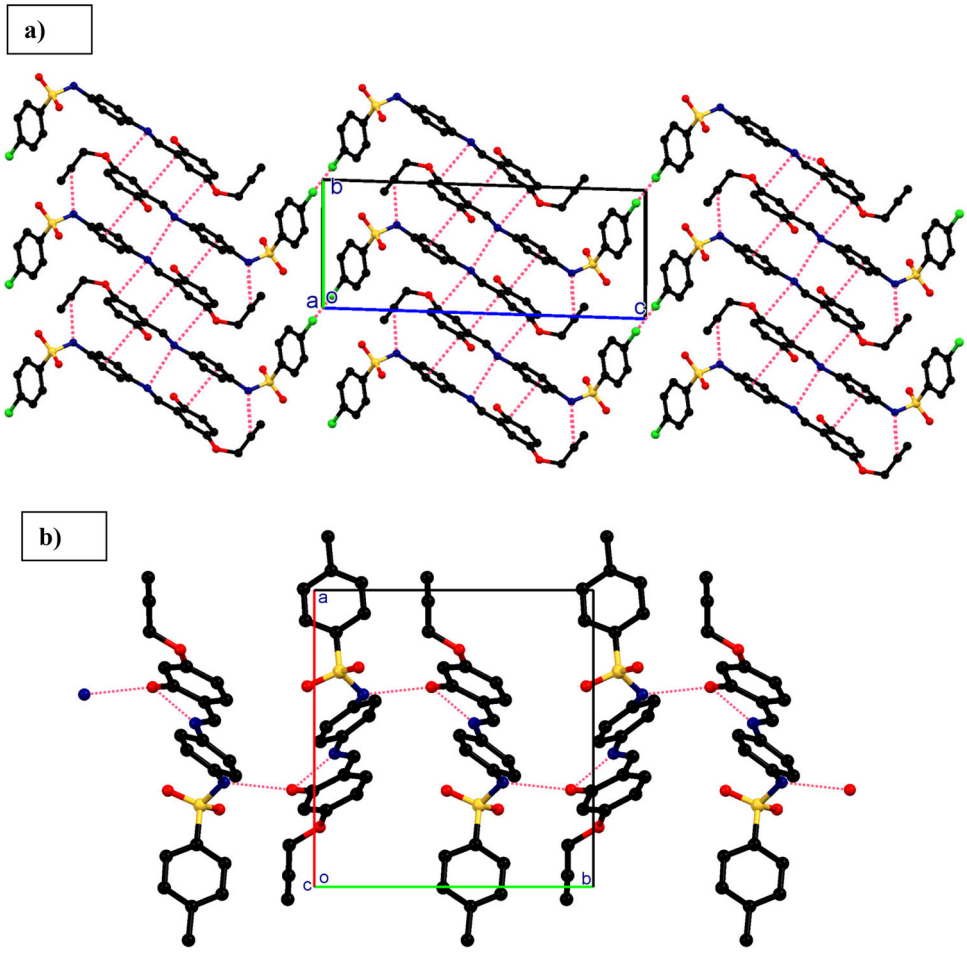

Figure 4. (a) Packing diagram of **6** viewing down the *a* axis showing. The π–π stacking interactions are shown as dashed lines. (b) Packing diagram of **7** viewing down the *bc* axis showing hydrogen bond chain.

Table 3. The electronic spectral data for compounds **3**–**8** in the solution and solid state.

	(λ_{max})	
Compounds	Solution (MeOH) λ (ε)	Solid state
3	240(0.31×10^5), 290(0.05×10^5)	235, 290
4	240(0.18×10^5), 295(0.02×10^5)	250, 290
5	240(0.11×10^5), 340(0.07×10^5), 430(0.03×10^5)	260, 340, 425
6	225(0.24×10^5), 280(0.16×10^5), 320(0.11×10^5), 360(0.11×10^5)	205, 295, 360
7	230(0.13×10^5), 340(0.10×10^5), 430(0.03×10^5)	235, 275, 345, 425
8	235(0.23×10^5), 285(0.10×10^5), 325(0.11×10^5), 370(0.10×10^5)	265, 365

8, the signal at 21.42 ppm may be assigned to the methyl group carbon atom of the sulfonamide fragment.

3.1. Molecular structure of compound 3

Perspective view of compound **3** is shown in Figure 1(a). The structure of compound **3** was solved in *orthorhombic* and space group $P2_12_12_1$. The compound contains two aromatic units, *para*-aminophenyl and *para*-chlorophenyl, connected by a $-SO_2NH$ (sulfonamide) functional bridge. The molecule is in U shape and two phenyl rings are inclined at 42.05(39)°. The S1–O1 and S1–O2 bond distances are 1.424(3) Å which is in the range of expected S = O double distances. S1–N1 and S1–C6 bond lengths of 1.614(4) and 1.754(5) Å, respectively, are comparable to those similar structures reported (Das et al., 2015; Mondal et al., 2015; Yildiz et al., 2010). The free amine group ($-NH_2$) and sulphony oxygen atoms are involved in intermolecular hydrogen bonds [$-NH_2\cdots O_2S-$ and NH·····N) forming a 2D hydrogen bond network along the *ab* axis (Figure 1(b)). The sulfonamide NH group also makes hydrogen bond with sulfony oxygen atom of an adjacent molecule forming a hydrogen bond chain. These 2D hydrogen bond sheets are further connected by hydrogen bond chains producing a 3D hydrogen bond supramolecular structure.

3.2. Molecular structures of compounds 5–7

Molecular structures of compounds **5**–**7** were investigated by single crystal X-ray diffraction studies. The structures of **5**

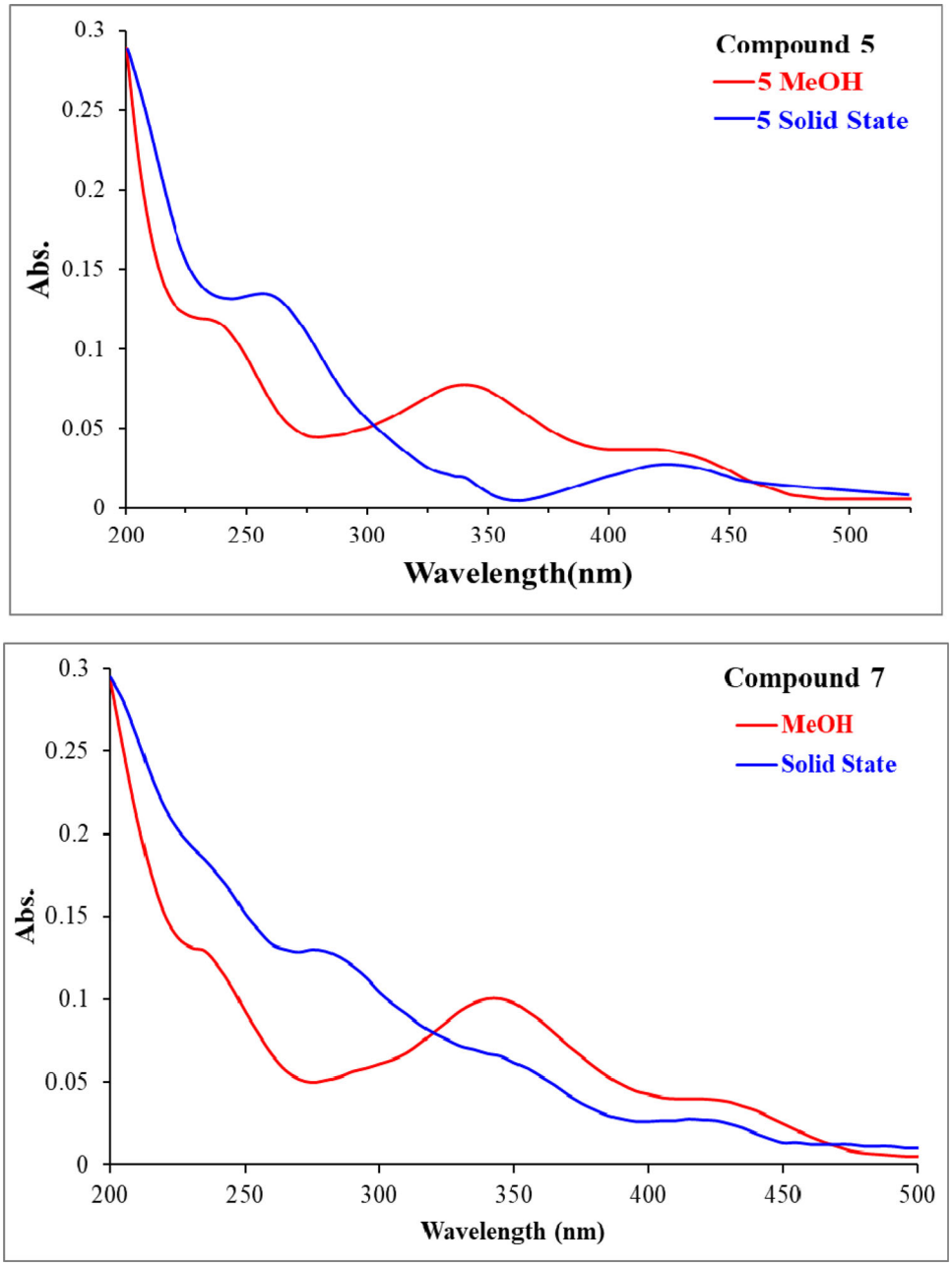

Figure 5. UV–vis spectra of compounds **5** and **7** in MeOH and solid state.

and **7** were solved in *monoclinic unit cell* and *P121/c1* space group (Table 1). Compound **6** crystallizes in *triclinic* unit cell and *P-1* space group. The structure of the three sulfonamide Schiff bases **5**–**7** contain a central phenyl ring linked to two outer phenyl and phenol rings by sulfonamide (–SO_2NH–) and azo-methine (–CH = N–) bridges.

The asymmetric unit of **5** has two independent molecules labelled as molecule A and B (Figure 2). The two independent molecules differ in the azomethine bond (–C13–N2 and –C13A–N2A) and phenolic (C15–O3 and C15A–O3A) bond distances and dihedral angles between the phenyl rings. In molecule A, the C13–N2 bond distance of 1.306(4) Å is relatively longer than usual C = N imine bond distance while C15–O3 distance of 1.299(4) Å is close to C = O double bond distance suggesting the keto-amine tautomeric form for molecule A (Table 2). However, in molecule B, C13A–N2A and shorter C15A–O3A bond distances are 1.293(4) and 1.321(4) Å, respectively, indicating the enol-imine tautomeric form for molecule B. For both independent molecules, the S–O distances are consistent with S = O double bonding. The O–S–O bond angles for molecules A and B are 118.31(17)° and 120.22(16)°, respectively, this values are considerably deviated from the value for ideal tetrahedral geometry due to the Thorpe–Ingold effect (Yildiz et al., 2010). The propargyl (–O–CH_2–C≡CH) and chloro-benzene ring are aligned opposite direction with respect to the almost planar phenyl–phenol rings. The phenyl (C7/C12) and phenol (C14/C19) rings in molecule A are almost co-planar with the twist angle of 5.49(21)°. However, in molecule B, the phenyl (C7A/C12A) and phenol (C14A/C19A) rings are considerably twisted from planarity with the dihedral angle of 36.76(14)°. Molecules A and B show intra-molecular NH·····O and OH·····N hydrogen

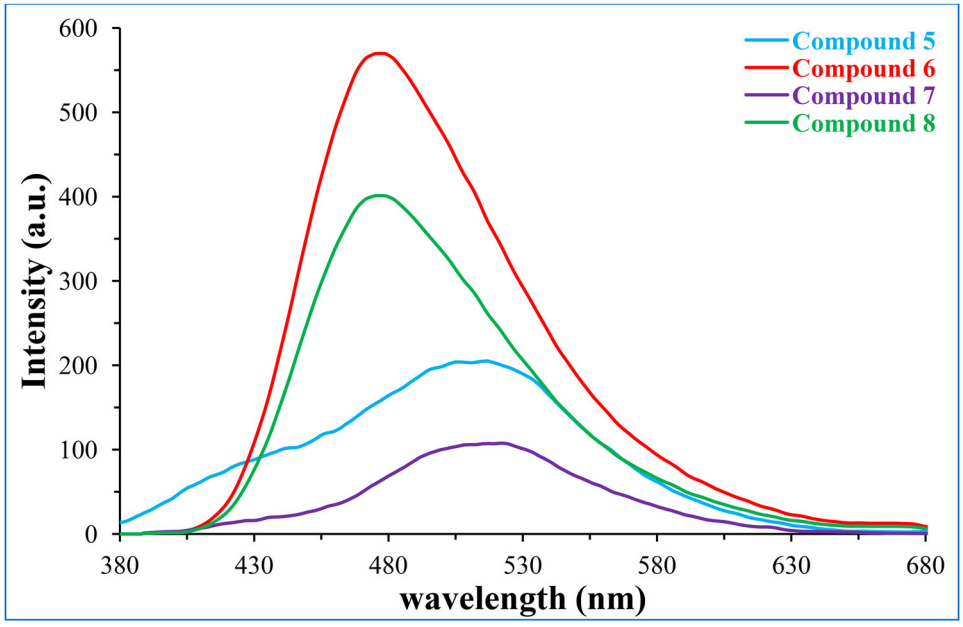

Figure 6. Emission spectra of compound **5**–**8** in MeOH (λ_{ex}: 340 nm for compound **5**, λ_{ex}: 320 nm for compound **6**, λ_{ex}: 345 nm for compound **7** and λ_{ex}: 330 nm for compound **8**).

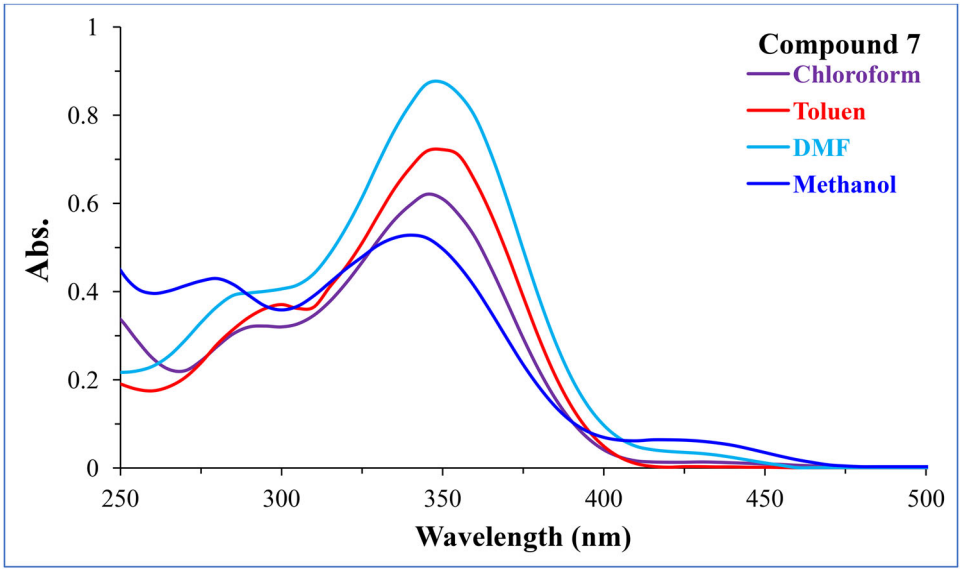

Figure 7. UV–vis spectra of compound **7** in different solvents.

bonds, respectively. In the structure of **5**, the NH group of sulfonamide makes hydrogen bond with the phenolic oxygen atom of an adjacent molecule forming a 1D hydrogen bond chain along the *b* axis (Figure 3(a)). The hydrogen bond chains are further linked by –C≡C–H·····O interactions forming 2D supramolecular structures. The almost co-planar phenyl and phenol rings in molecule A led the formation of the π–π stacking interactions with the same section of an adjacent molecule forming centro-symmetric π–π stacked dimers (Figure 3(b)). However, the similar stacking interactions were not observed for molecules with enol-imine tautomeric form.

Compound **7** exists in the enol-imine tautomeric form in the solid state (Figure 2). The C13–N2 and C15–O1 distances are 1.281(6) and 1.371(6) Å, respectively, showing the characteristic C = N (double bond) and C–O (single bond) distances. The geometry around sulphur atom of the sulfonamide is distorted tetrahedral and the O–S–O bond angle is 120.1(3)°. As seen in compound **5**, the propargyl (–O–CH_2–C≡CH) and chloro-benzene ring are located the opposite directions. In the molecule, the phenyl (C7/C12) and phenol (C14/C19) rings are slightly inclined with the dihedral angle of 4.214(28)°. The molecule shows an expected intra-molecular phenol-imine (O3–H·····N2). The molecules of **6** are arranged in head-to-tail columns *via* π–π stacking interactions. The sulfonamide (–SO_2NH–) groups do not involve hydrogen bonding interactions between the neighbouring molecules. The NH·····$C_{propargyl}$ contacts support the π–π stacking

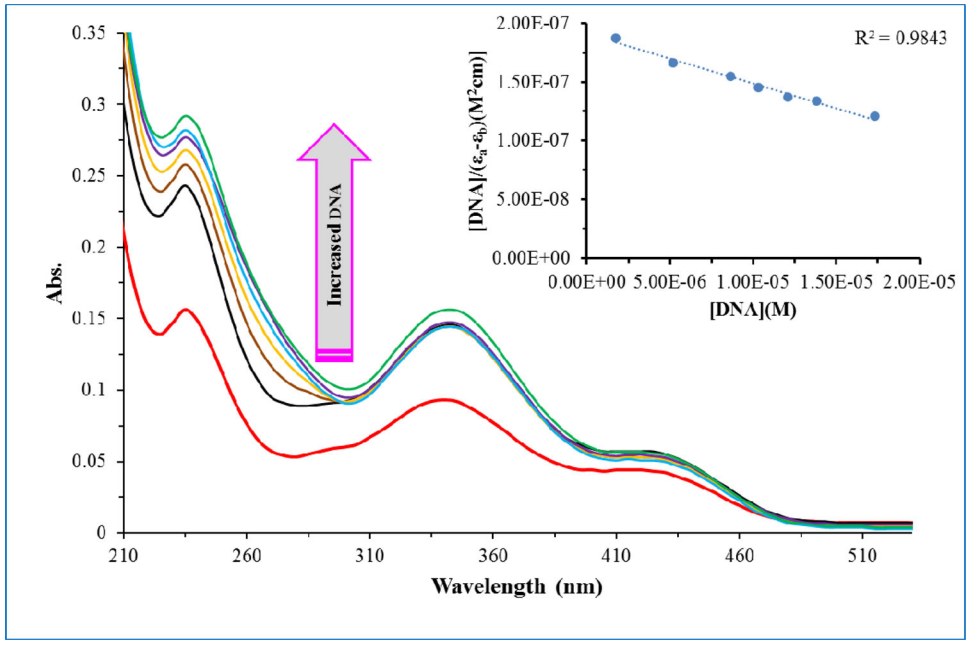

Figure 8. UV–vis spectral change of **5** upon incremental addition of FSdsDNA.

interactions. The head-to-tail columns are further linked by halogen bond type interactions (Cl·····Cl distance is 3.417 Å (Figure 4(a)).

The structure of compound **7** (Figure 2) is similar to that compound **5** differing in the substitute group on the phenyl ring (C1/C6). The X-ray crystallographic data showed that the compound crystallizes in the keto-amine tautomeric form in the solid state. The C13–N2 distance of 1.310(3) Å is longer than characteristic C = N bond distance. On the other hand, C15–O1 distance (1.296(2) Å) is shorter than that of usual Ph–O bond distance confirming the keto-amine form. The structural parameters for the sulfonamide (–SO_2NH–) group (geometry around sulphur atom and S–O bond distances) of compound **7** are similar to that of compound **5**. The phenyl (C7/C12) and phenol (C14/C19) rings are slightly twisted from planarity with the dihedral angle of 10.05(13)°. In the structure of **7**, there is N2–H·····O3 intramolecular hydrogen bond. The molecules of **7** form one dimensional head-to-tail hydrogen bond chains (–SO_2NH·····O_{phenol}) along the *bc* axis (Figure 4(b)). The hydrogen bond chains are further linked by the π–π stacking interactions. The phenyl (C7/C12) and phenol (C14/C19) rings are stacked with the same section of an adjacent molecule forming centro-symmetric dimers.

3.3. Photophysical properties

The UV–vis absorption properties of compounds **3**–**8** were investigated in the CH_3OH and solid state. The obtained spectral data are given in Table 3. The UV–vis spectra of compounds **5** and **7** are given in Figure 5 and rest of the spectra are provided in the Supplementary File. Compounds **3** and **4** in the solid state and CH_3OH solution have two absorption bands in the range 235–290 and 240–295 nm, respectively. These bands may be assigned to the π–π* and n–π* transitions. On the other hand, compounds **5**–**8** have three or four bands in the range 225–430 and 205–425 nm. When the spectral and reflectance values obtained from in the methanol solution medium and solid state of the compounds are compared; it was determined that the absorbance values in the methanol solvent medium shifted to longer wavelengths due to the solvent effect (hydrogen bonding between solute and solvent). As different from the UV–vis spectra of **6** and **8** both in MeOH and solid state, compounds **5** and **7** showed an absorption band with lower absorbance values in the range of 400–450 nm. The appearance of this band may be due to the tautomeric transformation from enol-imine to keto-amine form (Gözel et al., 2014; Köse et al., 2013). The X-ray crystallographic data also confirmed that compounds **5** and **7** favour the keto-amine tautomeric form in the solid state.

Table 4. Intrinsic binding (K_b) and quenching *Ksv* constants for compounds **5**–**8**.

Compounds	K_b (M^{-1})	*Ksv* (M^{-1})
5	2.10×10^4	2.88×10^4
6	2.40×10^4	2.00×10^4
7	3.90×10^4	1.00×10^4
8	3.10×10^4	1.58×10^4

The emission spectral properties of the *N*-(4-aminophenyl)-4-chloro-benzene sulfonamide (**3**), *N*-(4-aminophenyl)-4-methylbenzenesulfonamide (**4**) and their condensation products **5**–**8** have been investigated in the methanol solution (1.0×10^{-3} M). The inner filter effect in the fluorescence intensities were eliminated using absorption of the exciting light and reabsorption of emitted light (Rashidipour et al., 2016). The emission spectra of compounds **5**–**8** are given in Figure 6. The starting sulfonamide compounds **3** and **4** in the solution show the emission bands at 408 and 407 nm, respectively. On the other hand, the emission spectra of compounds **5**–**8** in the methanol solution have shifted to higher wavelengths in the

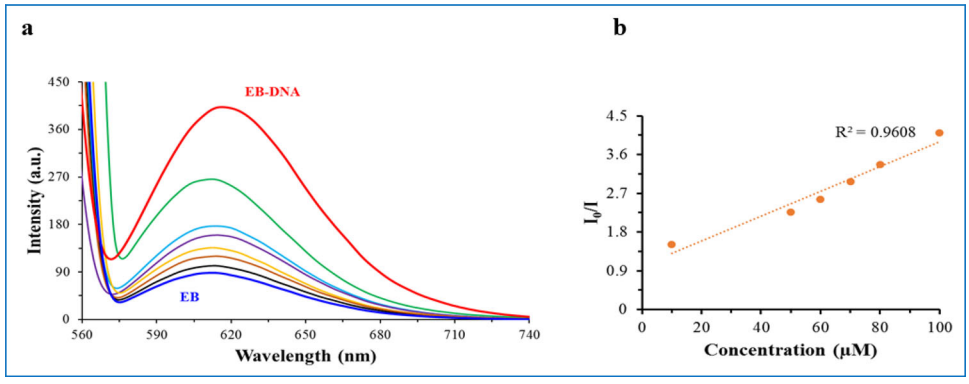

Figure 9. Effect of addition of **5** (a) the emission intensity of the FSdsDNA-bound ethidium bromide (75 μM) at different concentrations (0–65 μM) in 2 mM Tris-HCl buffer (pH 7.1) (λ_{ex}: 526 nm for **EB**–**DNA**), (b) Stern–Volmer plot of fluorescence titrations of the complexes with FSdsDNA.

475–517 nm range. Compounds **5** and **7** are the most shifting to long wavelengths. In the structure of these compounds, the propargyl group is in the 4-position relative to the carbonyl group and attracts electrons from the ring. Another important point is that these molecules exhibit tautomeric properties by the movement of π-electrons. Stokes shift is the difference between absorption and emission maxima and occurs due to structural relaxation in the excited state. In short, it reflects the difference between the equilibrium geometries of the fundamental and excited states. Compounds with the highest Stokes shift are the sulfa derivatives **5** and **7**.

Compounds **5–8** have the potential to show tautomer properties in different solvents. In order to further investigate the effect of the solvent on the tautomeric transformation of compounds **5** and **7**, the electronic spectral properties were studied in DMF, methanol, chloroform and toluene. The spectra obtained for compound **7** are given in Figure 7. Compounds **5** and **7** have one absorption band at 400–450 nm range in MeOH and DMF which are polar solvents. This relatively weak absorption bands may be due to the keto-amine tautomeric formation in these solutions. However, this band was not observed in toluene and chloroform confirming the solvent dependent tautomeric transformation for compounds **5** and **7**.

3.4. DNA binding studies

To examine the interaction between the synthesized compounds (**5**–**8**) and FSdsDNA, UV–vis spectral changes of the compounds were monitored upon addition of DNA. The spectral change of compound **5** upon addition of DNA is shown in Figure 8 and rest of the spectra are provided in the Supplementary Documents. The compounds showed three absorption bands in the range of 210–500 nm due to the π–π* and n–π* electronic transitions. The addition DNA to the solution of **5**–**8** increased the intensity of the all three absorption bands (hyperchromic effect). However, the most obvious increase was observed for π–π* transition in the range of 210–260 nm. The gradual increase was observed in the absorption band of π–π* transition by the incremental addition of the DNA solution. The hyperchromism has been often referred to the damage in the DNA double-helix structure due to the electrostatic binding or to partial uncoiling of the helix structure of DNA (Anjomshoa et al., 2014; Vijayalakshmi et al., 2000). This increase showed a linear curve (1×10^{-5} and 5×10^{-5} M DNA concentration range). Moreover, the interactions between the binder molecules **5**–**8** and DNA resulted in hyperchromism with no change in the position of bands.

Based on the absorbance values obtained from the UV–vis spectroscopic titration, the intrinsic DNA binding constant, K_b, was calculated according to the equation reported in literature (Tumer et al., 2017). The K_b binding constants of compounds **5**–**8** are given in Table 4. The sulfonamide-based compounds showed similar binding constants and these are close to the binding affinity of the intercalating agent, ethidium bromide ($K_b = 1.23 \pm 0.07 \times 10^5$ M^{-1}) (Psomas, 2008). The order of the binding efficiency of compounds is **8** > **6** > **5** > **7**.

According to the UV–vis titration experiments, K_b values were found to be around 10^4 M^{-1}, which shows the non-intercalative binding (Kamshad et al., 2019). The affinity of intercalating agents is very high with K_b around 10^5 to 10^6 M^{-1}. Moreover, only the molecules with planar aromatic rings involve in intercalation between DNA base pairs. Non-planar nature of the compounds also shows the non-intercalative binding with DNA (Howe-Grant et al., 1976; Sehlstedt et al., 1994).

To further examine the interaction between the sulfonamide-based compounds **5–8** and FSdsDNA, competitive binding experiments with DNA was carried out. Ethidium bromide, a standard DNA inter chelating agent, shows very weak emission in the range of 560–680 nm when excited 340 nm. However, the emission intensity of EB increases significantly upon interaction with DNA (Bera et al., 2008; Qais et al., 2017). The gradual addition of compounds **5**–**8** to the EB–DNA complex cause a decrease in the emission band (quenching effect) (Figure 9). The quenching of the emission band of the EB–DNA complex can be assigned to the non-displacement based quenching due to the enhanced energy transfer, either from excited ethidium to an acceptor or from a donor to an excited ethidium acceptor (Arabzadeh et al., 2002; Bathaie et al., 2007; Pasternack et al., 1991). The

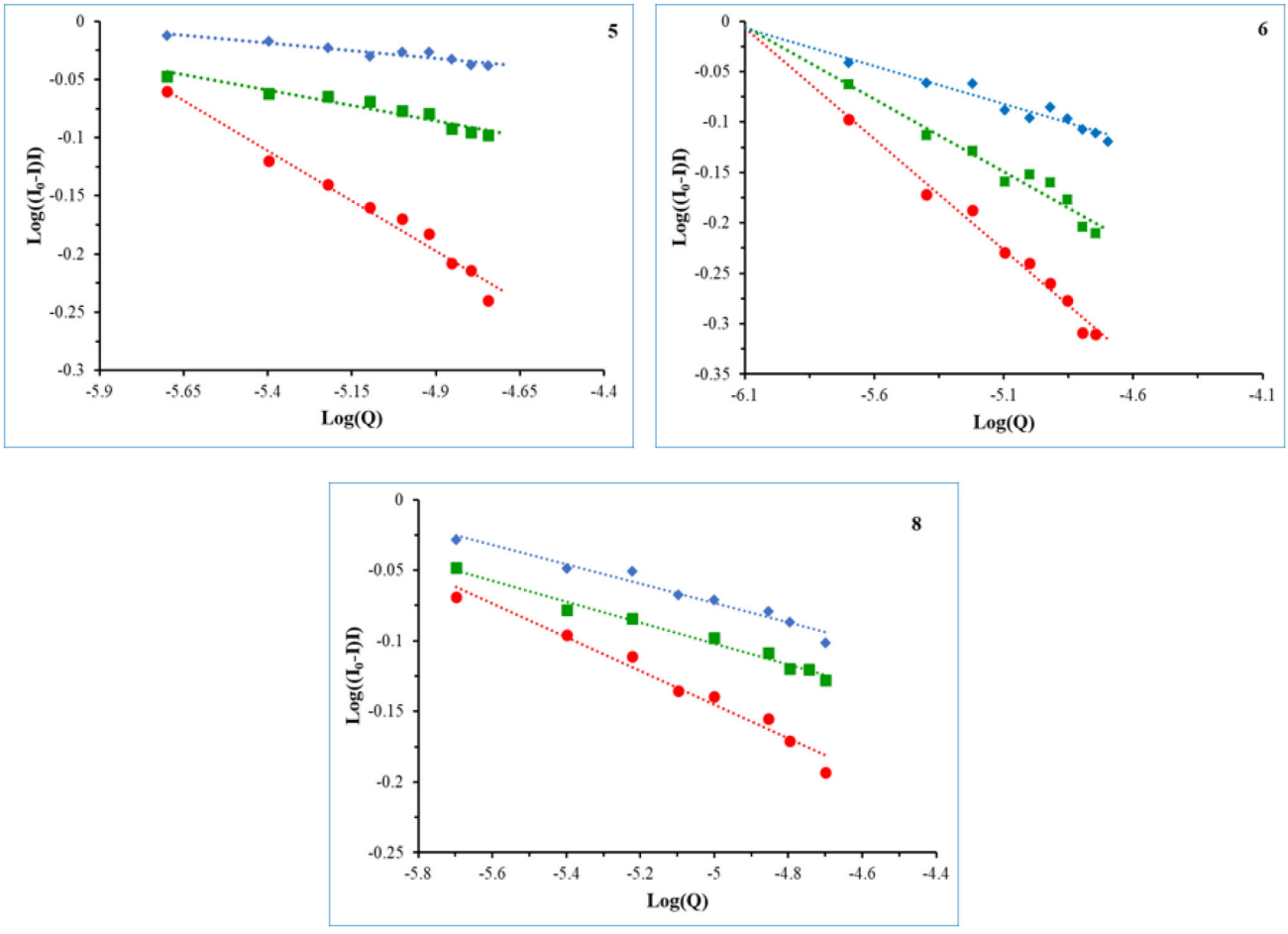

Figure 10. Competition between compounds **5**–**8** with ethidium bromide for the binding sites of FSdsDNA (Scatchard plot). In curves nos. 50 μM (●), 100 μM (■), 150 μM (◆), respectively, **5**, **6** and **8** at room temperature were added.

fluorescence quenching data were analysed by the Stern–Volmer equation and the quenching constants (K_{sv}) were calculated. The compounds showed very similar quenching efficiencies and the substitute groups (chloro or methyl) on benzene sulfonamide unit and positions of the propargyl arm did not have considerable effect on the DNA binding properties of the molecules.

In order to further investigate the binding mode of the compounds with DNA, the Scatchard plots of the binding of EtBr to DNA in the absence and presence of compounds **5**–**8** were obtained by fluorometric data (Figure 10 and Table 5). The X-ray crystallographic data showed that compounds **5**–**8** lack planar aromatic rings. Therefore, the compounds are not good candidates for intercalation between DNA base pairs. The changes in both K and n revealed the non-competitive inhibitory manner of the ligand in Et-DNA interaction (Arabzadeh et al., 2002; Bathaie et al., 2007).

Table 5. Binding parameters for compounds **5**–**8** on the fluorescence of EBr in the presence of CT-DNA.

Compound	r_f	K	n
5	0.83	0.156	0.9311
	0.166	0.1329	0.8145
	2.5	0.1426	0.9017
6	0.83	0.1431	0.8621
	0.166	0.1386	0.8396
	2.5	0.124	0.8124
8	0.83	0.068	0.4154
	0.166	0.071	0.48.13
	2.5	0.083	0.5636

3.5. Molecular docking studies

Molecular docking studies are a technological perspective of today's drug discovery. It is also an important technique in illuminating the type of interaction of the drug candidate with the selected target protein. Knowing the physics of interaction of drug candidates with DNA today can convey striking information in the application and development of the drug candidate. The preferred place of the examined **5**–**8** compounds on fish sperm DNA (PDB ID: 423 D) (Jamshidvand et al., 2018) and their binding energies, type of interaction and nucleotides in the binding sites resulting from their interaction with DNA are given in Table 6. The molecular docking and the binding site of compounds **5**–**8** interacting with DNA are shown in Figure 11. According to the results of the docking, the compounds considered as drug candidates settled in the groove of DNA. The interaction energy obtained with molecular docking were quite consistent with experimental binding constants. The docked models suggest that the synthesized compounds **5**–**8** interact with the minor groove of DNA with binding energy of −8.45, −8.55, −8.76 and −8.69 kcal/mol, respectively. The

Table 6. Molecular docking result data of compound **5**–**8** with 423 D.

Compounds	Binding energy (kcal/mol)	Bases around molecules	H-bond	π–π interaction
5	−8.45	DG7, DT8, DC9, DG10, DG11, DG16, DA17, DC18, DG19	DG7 (2.6 Å), DG10 (2.0 Å, 2.2 Å), DG16 (3.0 Å), DA17 (2.1 Å), DC18 (1.8 Å)	Yes
6	−8.55	DG7, DT8, DC9, DG10, DG11, DG16, DA17, DC18, DG19	DG10 (1.8 Å, 2.1 Å, 2.7 Å), DG16 (1.9 Å, 2.1 Å), DA17 (2.3 Å), DC18 (1.9 Å)	Yes
7	−8.76	DC6, DG7, DT8, DC9, DG10, DG11, DG16, DA17, DC18, DG19	DG7 (2.7 Å), DG10 (1.8 Å, 2.7 Å, 3.0 Å), DG16 (1.8 Å, 3.0 Å), DA17 (2.6 Å), DC18 (2.1 Å, 2.6 Å)	Yes
8	−8.69	DG7, DT8, DC9, DG10, DG11, DG16, DA17, DC18, DG19	DG7 (2.9 Å), DG10 (1.8 Å, 2.8 Å), DG16 (1.9 Å, 2.4 Å, 2.9 Å), DA17 (2.2 Å), DC18 (2.1 Å)	Yes

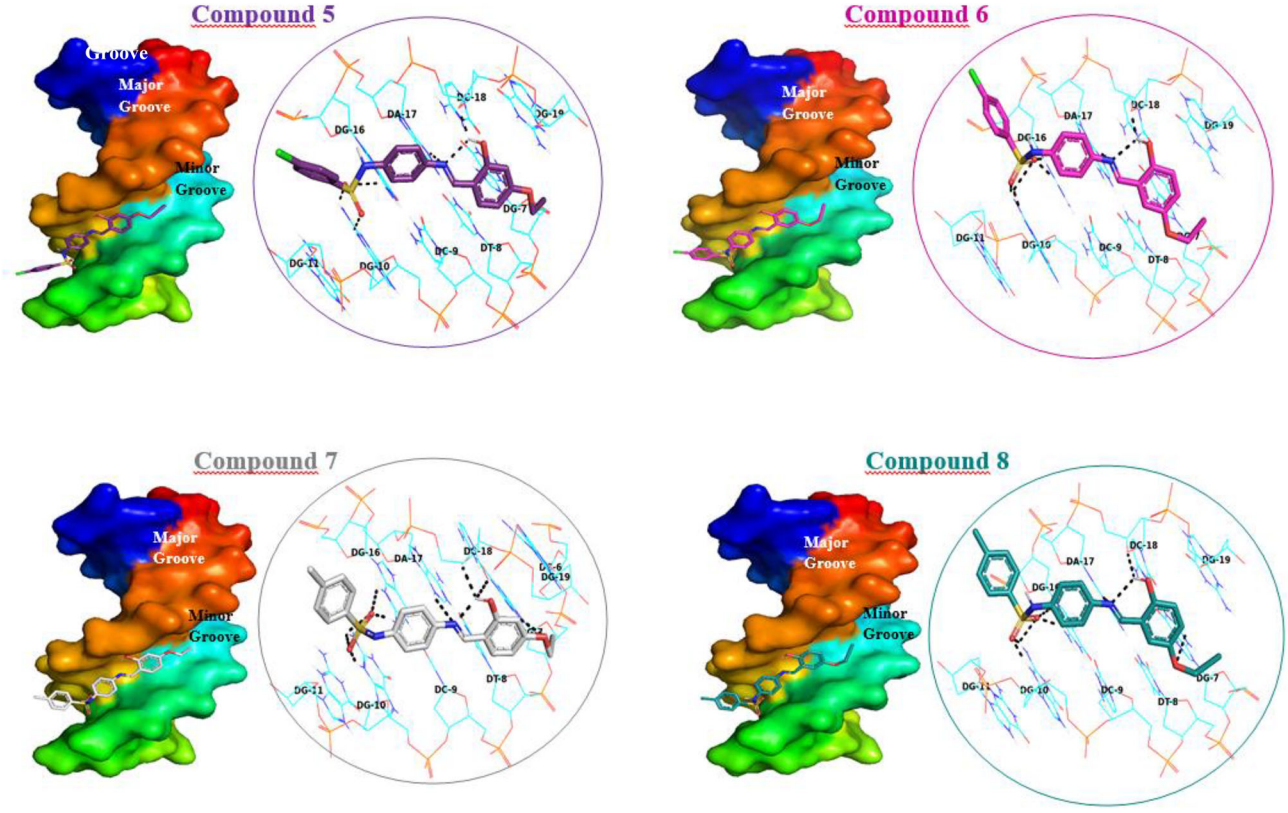

Figure 11. Molecular docking pose showing the potential interactions of compound **5**–**8** with 423 D.

binding energy of compounds **5**–**8** with DNA are consistent with experimental values (Dehghani Sani et al., 2018; Shakibapour et al., 2019). However, binding energy of the compounds are higher than those intercalation agents reported in literature which also suggests non-intercalative binding of compounds with DNA.

According to the free binding energies, compound **7** showed the best interaction with DNA. In addition, compound **7** appear to be fixed on DNA by forming H-bond and hydrophobic interactions. The number of interactions of compound **7** is higher than the number of interactions of other compounds. The backbone of all four compounds locates approximately same region of the minor groove of DNA. The sulfonamide oxygen atoms involved in strong hydrogen bond interactions with the DG10 and DG16 nucleotides of DNA. Alkyne groups in all compounds makes hydrophobic interactions with the DG7 nucleotide. Moreover, the compounds also make π–π stacking interactions with the DNA bases.

4. Conclusions

In the course of this work, four new sulfonamide-based Schiff base compounds **5**–**8** were prepared and characterized by common analytical and spectroscopic methods. The compounds favours either enol-imine or keto-amine tautomeric

form in the solid state. The absorption spectra of the compounds have also shown that these compounds can also exist in the both tautomeric form in solution depending on the solvent polarity. The compounds were screened for their binding affinity to the FSdsDNA and results showed that compounds have high binding affinity to the DNA compared to the ethidium bromine (a DNA intercalating agent). Finally, the interaction modes were investigated by molecular docking studies.

The experimental results from DNA binding studies as well as the molecular modeling, compounds **5**–**8** were able to interact with DNA *via* non-intercalative way with relatively high binding constants. These sulfonamide-based Schiff base compounds have potential to inhibit tumor growth. Moreover, this work will provide useful information to further understand the binding mechanism of small organic molecule with DNA and to design more efficient drug candidates targeting DNA.

Disclosure statement

No potential conflict of interest was reported by the authors.

Funding

Authors thank to the research unit of Kahramanmaras Sutcu Imam University for financial support of this work (Project number: 2019/1-17D).

ORCID

Seyit Ali Güngör http://orcid.org/0000-0002-3233-4529
Mehmet Tümer http://orcid.org/0000-0002-1882-429X
Muhammet Köse http://orcid.org/0000-0002-4597-0858
Sultan Erkan http://orcid.org/0000-0001-6744-929X

References

Anjomshoa, M., Fatemi, S. J., Torkzadeh-Mahani, M., & Hadadzadeh, H. (2014). DNA- and BSA-binding studies and anticancer activity against human breast cancer cells (MCF-7) of the zinc(II) complex coordinated by 5,6-diphenyl-3-(2-pyridyl)-1,2,4-triazine. *Spectrochimica Acta Part A: Molecular and Biomolecular Spectroscopy*, *127*, 511–520. https://doi.org/10.1016/j.saa.2014.02.048

Arabzadeh, A., Bathaie, S. Z., Farsam, H., Amanlou, M., Saboury, A. A., Shockravi, A., & Moosavi-Movahedi, A. A. (2002). Studies on mechanism of 8-methoxypsoralen–DNA interaction in the dark. *International Journal of Pharmaceutics*, *237*(1–2), 47–55. https://doi.org/10.1016/s0378-5173(02)00020-0

Basak, D., & Ray, D. (2020). Metal ion substitution and aldehyde exchange for CuII4 aggregates from two types of piperazine-based Schiff base ligands: Synthesis, X-ray structures, magnetic studies and theoretical validation. *Inorganica Chimica Acta*, *503*, 119439. https://doi.org/10.1016/j.ica.2020.119439

Bathaie, S. Z., Bolhasani, A., Hoshyar, R., Ranjbar, B., Sabouni, F., & Moosavi-Movahedi, A. A. (2007). Interaction of saffron carotenoids as anticancer compounds with ctDNA, oligo (dG.dC)15, and oligo (dA.dT)15. *DNA and Cell Biology*, *26*(8), 533–540. https://doi.org/10.1089/dna.2007.0598

Bera, R., Sahoo, B. K., Ghosh, K. S., & Dasgupta, S. (2008). Studies on the interaction of isoxazolcurcumin with calf thymus DNA. *International Journal of Biological Macromolecules*, *42*(1), 14–21. https://doi.org/10.1016/j.ijbiomac.2007.08.010

Boer, D. R., Canals, A., & Coll, M. (2009). DNA-binding drugs caught in action: The latest 3D pictures of drug–DNA complexes. *Dalton Transactions*, *3*, 399–414.

Das, D., Sahu, N., Roy, S., Dutta, P., Mondal, S., Torres, E. L., & Sinha, C. (2015). The crystal structure of sulfamethoxazole, interaction with DNA, DFT calculation, and molecular docking studies. *Spectrochimica Acta Part A: Molecular and Biomolecular Spectroscopy*, *137*, 560–568. https://doi.org/10.1016/j.saa.2014.08.034

Davenport, D. (2012). The war against bacteria: How were sulphonamide drugs used by Britain during World War II? *Medical Humanities*, *38*(1), 55–58. https://doi.org/10.1136/medhum-2011-010024

Dehghani Sani, F., Shakibapour, N., Beigoli, S., Sadeghian, H., Hosainzadeh, M., & Chamani, J. (2018). Changes in binding affinity between ofloxacin and calf thymus DNA in the presence of histone H1: Spectroscopic and molecular modeling investigations. *Journal of Luminescence*, *203*(June), 599–608. https://doi.org/10.1016/j.jlumin.2018.06.083

Dixit, R. B., Patel, T. S., Vanparia, S. F., Kunjadiya, A. P., Keharia, H. R., & Dixit, B. C. (2011). DNA-binding interaction studies of microwave assisted synthesized sulfonamide substituted 8-hydroxyquinoline derivatives. *Scientia Pharmaceutica*, *79*(2), 293–308. https://doi.org/10.3797/scipharm.1102-16

Doğan, S., Tümay, S. O., Mutlu Balci, C., YeŞİlot, S., & BeŞİl, S. (2020). Synthesis of new cyclotriphosphazene derivatives bearing Schiff bases and their thermal and absorbance properties. *Turkish Journal of Chemistry*, *44*(1), 31–47. https://doi.org/10.3906/kim-1905-60

Drews, J. (2000). Drug discovery: A historical perspective. *Science (New York, N.Y.)*, *287*(5460), 1960–1964. https://doi.org/10.1126/science.287.5460.1960

Durgun, M., Turkmen, H., Ceruso, M., & Supuran, C. T. (2016). Synthesis of 4-sulfamoylphenyl-benzylamine derivatives with inhibitory activity against human carbonic anhydrase isoforms I, II, IX and XII. *Bioorganic & Medicinal Chemistry*, *24*(5), 982–988. https://doi.org/10.1016/j.bmc.2016.01.020

Formica, M., Favi, G., Fusi, V., Giorgi, L., Mantellini, F., & Micheloni, M. (2018). Synthesis and study of three hydroxypyrazole-based ligands: A ratiometric fluorescent sensor for Zn(II). *Journal of Luminescence*, *195*, 193–200. https://doi.org/10.1016/j.jlumin.2017.11.018

García-Giménez, J. L., Hernández-Gil, J., Martínez-Ruíz, A., Castiñeiras, A., Liu-González, M., Pallardó, F. V., Borrás, J., & Alzuet Piña, G. (2013). DNA binding, nuclease activity, DNA photocleavage and cytotoxic properties of Cu(II) complexes of N-substituted sulfonamides. *Journal of Inorganic Biochemistry*, *121*, 167–178. https://doi.org/10.1016/j.jinorgbio.2013.01.003

Golcu, A., Tumer, M., Demirelli, H., & Wheatley, R. A. (2005). Cd(II) and Cu(II) complexes of polydentate Schiff base ligands: Synthesis, characterization, properties and biological activity. *Inorganica Chimica Acta*, *358*(6), 1785–1797. https://doi.org/10.1016/j.ica.2004.11.026

Gözel, A., Kose, M., Karakaş, D., Atabey, H., McKee, V., & Kurtoglu, M. (2014). Spectral, structural and quantum chemical computational and dissociation constant studies of a novel azo-enamine tautomer. *Journal of Molecular Structure*, *1074*, 449–456. https://doi.org/10.1016/j.molstruc.2014.06.033

Güngör, S. A., Tümer, M., Köse, M., & Erkan, S. (2020). Benzaldehyde derivatives with functional propargyl groups as α-glucosidase inhibitors. *Journal of Molecular Structure*, *1206*, 127780.

Henry, R. J. (1943). The mode of action of sulfonamides. *Bacteriological Reviews*, *7*(4), 175–262. https://doi.org/10.1128/BR.7.4.175-262.1943

Horiuchi, H. (2002). Molecular structure of nuclei. *The European Physical Journal A*, *15*(1–2), 131–133. https://doi.org/10.1140/epja/i2001-10240-x

Howe-Grant, M., Lippard, S. J., Wu, K. C., & Bauer, W. R. (1976). Binding of platinum and palladium metallointercalation reagents and antitumor drugs to closed and open DNAs. *Biochemistry*, *15*(19), 4339–4346. https://doi.org/10.1021/bi00664a031

Jaiswal, M., Khadikar, P. V., & Supuran, C. T. (2004). Topological modeling of lipophilicity, diuretic activity, and carbonic inhibition activity of benzene sulfonamides: A molecular connectivity approach. *Bioorganic*

& *Medicinal Chemistry Letters*, *14*(22), 5661–5666. https://doi.org/10.1016/j.bmcl.2004.08.051

Jamshidvand, A., Sahihi, M., Mirkhani, V., Moghadam, M., Mohammadpoor-Baltork, I., Tangestaninejad, S., Amiri Rudbari, H., Kargar, H., Keshavarzi, R., & Gharaghani, S. (2018). Studies on DNA binding properties of new Schiff base ligands using spectroscopic, electrochemical and computational methods: Influence of substitutions on DNA-binding. *Journal of Molecular Liquids*, *253*, 61–71. https://doi.org/10.1016/j.molliq.2018.01.029

Kamshad, M., Jahanshah Talab, M., Beigoli, S., Sharifirad, A., & Chamani, J. (2019). Use of spectroscopic and zeta potential techniques to study the interaction between lysozyme and curcumin in the presence of silver nanoparticles at different sizes. *Journal of Biomolecular Structure and Dynamics*, *37*(8), 2030–2040. https://doi.org/10.1080/07391102.2018.1475258

Köse, M., Kurtoglu, N., Gümüşsu, Ö., Tutak, M., McKee, V., Karakaş, D., & Kurtoglu, M. (2013). Synthesis, characterization and antimicrobial studies of 2-{(E)-[(2-hydroxy-5-methylphenyl)imino]methyl}-4-[(E)-phenyldiazenyl]phenol as a novel azo-azomethine dye. *Journal of Molecular Structure*, *1053*, 89–99. https://doi.org/10.1016/j.molstruc.2013.09.013

Krátký, M., Vinšová, J., Volková, M., Buchta, V., Trejtnar, F., & Stolaříková, J. (2012). Antimicrobial activity of sulfonamides containing 5-chloro-2-hydroxybenzaldehyde and 5-chloro-2-hydroxybenzoic acid scaffold. *European Journal of Medicinal Chemistry*, *50*, 433–440. https://doi.org/10.1016/j.ejmech.2012.01.060

Marchetti, F., Pettinari, C., Di Nicola, C., Tombesi, A., & Pettinari, R. (2019). Coordination chemistry of pyrazolone-based ligands and applications of their metal complexes. *Coordination Chemistry Reviews*, *401*, 213069. https://doi.org/10.1016/j.ccr.2019.213069

Marchetti, F., Pettinari, R., & Pettinari, C. (2015). Recent advances in acylpyrazolone metal complexes and their potential applications. *Coordination Chemistry Reviews*, *303*, 1–31. https://doi.org/10.1016/j.ccr.2015.05.003

Mokaberi, P., Babayan-Mashhadi, F., Amiri Tehrani Zadeh, Z., Saberi, M. R., & Chamani, J. (2020). Analysis of the interaction behavior between nano-curcumin and two human serum proteins: Combining spectroscopy and molecular stimulation to understand protein–protein interaction. *Journal of Biomolecular Structure and Dynamics*, *0*(0), 1–20.

Mondal, S., Bhanja, A. K., Ojha, D., Mondal, T. K., Chattopadhyay, D., & Sinha, C. (2015). Fluorescence sensing and intracellular imaging of Al3+ ions by using naphthalene based sulfonamide chemosensor: Structure, computation and biological studies. *RSC Advances*, *5*(90), 73626–73638. https://doi.org/10.1039/C5RA11548E

Pahontu, E., Julea, F., Rosu, T., Purcarea, V., Chumakov, Y., Petrenco, P., & Gulea, A. (2015). Antibacterial, antifungal and in vitro antileukaemia activity of metal complexes with thiosemicarbazones. *Journal of Cellular and Molecular Medicine*, *19*(4), 865–878. https://doi.org/10.1111/jcmm.12508

Pasternack, R. F., Caccam, M., Keogh, B., Stephenson, T. A., Williams, A. P., & Gibbs, E. J. (1991). Long-range fluorescence quenching of ethidium ion by cationic porphyrins in the presence of DNA. *Journal of the American Chemical Society*, *113*(18), 6835–6840. https://doi.org/10.1021/ja00018a019

Psomas, G. (2008). Mononuclear metal complexes with ciprofloxacin: Synthesis, characterization and DNA-binding properties. *Journal of Inorganic Biochemistry*, *102*(9), 1798–1811. https://doi.org/10.1016/j.jinorgbio.2008.05.012

Qais, F. A., Abdullah, K. M., Alam, M. M., Naseem, I., & Ahmad, I. (2017). Interaction of capsaicin with calf thymus DNA: A multi-spectroscopic and molecular modelling study. *International Journal of Biological Macromolecules*, *97*, 392–402. https://doi.org/10.1016/j.ijbiomac.2017.01.022

Rajendiran, N., & Thulasidhasan, J. (2015). Interaction of sulfanilamide and sulfamethoxazole with bovine serum albumin and adenine: Spectroscopic and molecular docking investigations. *Spectrochimica Acta Part A: Molecular and Biomolecular Spectroscopy*, *144*, 183–191. https://doi.org/10.1016/j.saa.2015.01.127

Rashidipour, S., Naeeminejad, S., & Chamani, J. (2016). Study of the interaction between DNP and DIDS with human hemoglobin as binary and ternary systems: Spectroscopic and molecular modeling investigation. *Journal of Biomolecular Structure & Dynamics*, *34*(1), 57–77. https://doi.org/10.1080/07391102.2015.1009946

Sehlstedt, U., Nordén, B., Kim, S. K., Carter, P., Goodisman, J., Dabrowiak, J. C., & Vollano, J. F. (1994). Interaction of cationic porphyrins with DNA. *Biochemistry*, *33*(2), 417–426. https://doi.org/10.1021/bi00168a005

Shakibapour, N., Dehghani Sani, F., Beigoli, S., Sadeghian, H., & Chamani, J. (2019). Multi-spectroscopic and molecular modeling studies to reveal the interaction between propyl acridone and calf thymus DNA in the presence of histone H1: Binary and ternary approaches. *Journal of Biomolecular Structure and Dynamics*, *37*(2), 359–371. https://doi.org/10.1080/07391102.2018.1427629

Tajudeen, S. S., & Kannappan, G. (2016). Indian journal of advances in chemical science Schiff base – copper (II) complexes: Synthesis, spectral studies and anti-tubercular and antimicrobial activity. *Indian Journal of Advances in Chemical Science*, *4*(1), 40–48.

Tumer, F., Golcu, A., Tumer, M., Bulut, S., & Kose, M. (2017). Multifunctional metallo porphyrin-imine conjugates: Photophysical, electrochemical, DNA binding and SOD enzyme mimetic studies. *Journal of Photochemistry and Photobiology A: Chemistry*, *346*, 236–248. https://doi.org/10.1016/j.jphotochem.2017.06.010

Vijayalakshmi, R., Kanthimathi, M., Subramanian, V., & Nair, B. U. (2000). Interaction of DNA with [Cr (Schi ¡ base) $(H_2O)_2$] ClO_4. *Science*, *1475*, 157–162.

Wang, J., Zhang, X., Liu, H. B., Zhang, D., Nong, H., Wu, P., Chen, P., & Li, D. (2020). Aggregation induced emission active fluorescent sensor for the sensitive detection of Hg2+ based on organic–inorganic hybrid mesoporous material. *Spectrochimica Acta Part A: Molecular and Biomolecular Spectroscopy*, *227*, 117585. https://doi.org/10.1016/j.saa.2019.117585

Wei, Z. L., Wang, L., Guo, S. Z., Zhang, Y., & Dong, W. K. (2019). A high-efficiency salamo-based copper(II) complex double-channel fluorescent probe. *RSC Advances*, *9*(70), 41298–41304. https://doi.org/10.1039/C9RA09017G

Xing, L., Zheng, X., Sun, W., Yuan, H., Hu, L., & Yan, Z. (2018). UV–vis spectral property of a multi-hydroxyl Schiff-base derivative and its colorimetric response to some special metal ions. *Spectrochimica Acta Part A: Molecular and Biomolecular Spectroscopy*, *203*, 455–460. https://doi.org/10.1016/j.saa.2018.06.015

Yildiz, M., Ünver, H., Erdener, D., & Iskeleli, N. O. (2010). Spectroscopic studies and crystal structure of 4-(2-hydroxy-3-methoxybenzylideneamino)-N-(5-methylisoxazol-3-yl) benzenesulfonamide. *Journal of Chemical Crystallography*, *40*(8), 691–695. https://doi.org/10.1007/s10870-010-9723-9